Short-range Three-Nucleon Forces Effects on Nucleon-Deuteron Scattering

S. Ishikawa* [a] [b]

[a]Science Research Center, Hosei University, 2-17-1 Fujimi, Chiyoda, Tokyo 102-8160, Japan

[b]Triangle Universities Nuclear Laboratory, Durham, North Carolina 27708-0308, U.S.A.

Effects of three-nucleon forces arising from the exchange of a pion and a scalar-isoscalar object among three nucleons on nucleon-deuteron scattering observables are studied.

1. INTRODUCTION

The introduction of a three-nucleon force (3NF) arising from the exchange of two pions among three nucleons (2πE) as shown in Fig. 1 (a) into nuclear Hamiltonian is known to get rid of discrepancies between experimental data and theoretical calculations with realistic two-nucleon forces (2NFs) for the three-nucleon (3N) binding energies and nucleon-deuteron (ND) differential cross sections. On the other hand, the 2πE 3NF is unsuccessful in explaining some ND polarization observables, *e.g.*, too small effects to vector analyzing powers (VAPs) and undesirable contributions to tensor analyzing powers (TAPs) in low-energy ND elastic scattering (see Fig. 2).

In Refs. [4,5], we have pointed out that tensor components in the 2πE 3NF should be responsible to the problem in TAPs. In this paper, we examine a 3NF due to the exchange of a pion and a scalar-isoscalar object (π-S) shown in Fig. 1 (b) as a possible source of tensor interactions that have different characteristics from those of the 2πE 3NF.

After giving a general form of the π-S 3NF in Sec. 2, numerical results for the 3N binding energy and ND scattering observables will be presented in Sec. 3. Summary is given in Sec. 4.

2. PION-"SCALAR-ISOSCALAR-OBJECT" EXCHANGE THREE-NUCLEON FORCES

We will consider the following models for the π-S 3NFs: π-σ exchange with the excitation of the Roper resonance $N^*(1440)$ ($(\pi\text{-}\sigma)_{N^*}$) [6,7]; π-σ exchange corresponding to the nucleon Born diagrams (so called pair or Z diagrams) for the PV ($(\pi\text{-}\sigma)_{Z,PV}$) or the PS ($(\pi\text{-}\sigma)_{Z,PS}$) πNN coupling [6,7]; π-"effective scalar field" exchange by a linear model [8]

*Numerical calculations in this research were supported by Research Center for Computing and Multimedia Studies, Hosei University, under Project No. lab0003.

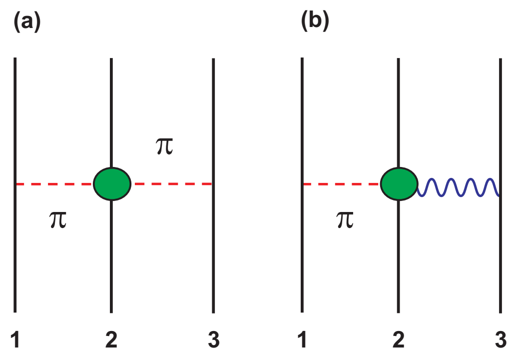

Figure 1. Diagrams for the 2πE 3NF (a) and the π-S 3NF (b). The wavy line between the nucleons 2 and 3 represents the exchange of a scalar-isoscalar object.

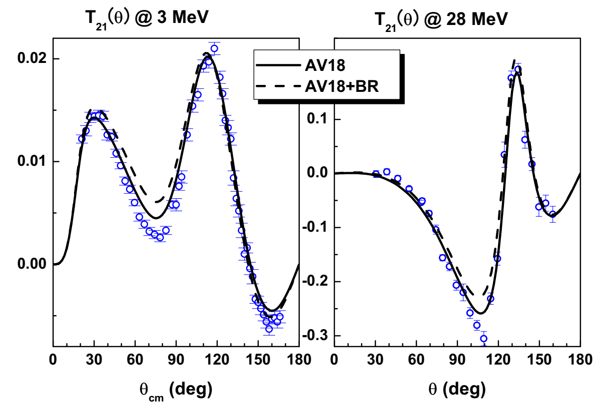

Figure 2. $T_{21}(\theta)$ of pd elastic scattering at $E = 3$ MeV and $E = 28$ MeV. The data are taken from Refs. [1,2] for 3 MeV and from Ref. [3] for 28 MeV.

or by a nonlinear model [8]; π-"effective 2π" exchange ((π-2π)) [9]. A coordinate space representation of these potentials corresponding to diagram Fig. 1 (b) is:

$$W_{12,3}\left(\boldsymbol{r}_{12}, \boldsymbol{r}_{32}\right) = (\vec{\tau}_1 \cdot \vec{\tau}_2)(\boldsymbol{\sigma}_1 \cdot \boldsymbol{\nabla}_{12})\Big[V_a(\boldsymbol{\sigma}_2 \cdot \boldsymbol{\nabla}_{12}) + V_b(\boldsymbol{\sigma}_2 \cdot \boldsymbol{\nabla}_{32})\Big] Y_\pi(r_{12}) Y_\sigma(r_{32}), \tag{1}$$

where $\boldsymbol{r}_{ij} = \boldsymbol{r}_j - \boldsymbol{r}_i$ with $\boldsymbol{r}_k$ being a position vector of nucleon k. When a dipole xNN form factor with a cutoff mass Λ_x is used, the function $Y_x(r)$ becomes $Y_x(r) = e^{-m_x r}/r - \{1 + (\Lambda_x^2 - m_x^2) r/(2\Lambda_x)\} e^{-\Lambda_x r}/r$. Expressions of V_a and V_b for the π-S 3NFs [6,7,8,9] are shown in Table 1.

Table 1
The potential strengths V_a and V_b for the π-S 3NF models and and effects of the 3NFs on the ^{3}H energy: $\Delta E_{3NF} \equiv E_{3,\mathrm{AV18+3NF}} - E_{3,\mathrm{AV18}}$.

	V_a	V_b	ΔE_{3NF} (MeV)
$(\pi\text{-}\sigma)_{N^*}$	$\frac{g_\pi g_\pi^*}{4\pi}\frac{g_\sigma g_\sigma^*}{4\pi}\frac{m_\pi^4}{2(m^*-m_N)m_N^2}$	–	-0.32
$(\pi\text{-}\sigma)_{Z,PV}$	–	$-\frac{g_\pi^2}{4\pi}\frac{g_\sigma^2}{4\pi}\frac{m_\pi^4}{4m_N^3}$	+0.47
$(\pi\text{-}\sigma)_{Z,PS}$	$\frac{g_\pi^2}{4\pi}\frac{g_\sigma^2}{4\pi}\frac{m_\pi^4}{4m_N^3}$	–	-1.04
Linear	$\left(\frac{g^2}{4\pi}\right)^2\frac{m_\pi^4}{4m_N^3}$	–	-1.99
Nonlinear	$\left(\frac{g^2}{4\pi}\right)^2\frac{m_\pi^4}{4m_N^3}\left(1-\frac{m_N}{gf_\pi}\right)$	$-\left(\frac{g^2}{4\pi}\right)^2\frac{m_\pi^4}{4m_N^3}\left(\frac{m_N}{gf_\pi}\right)$	+0.23
π-2π	$-\frac{g_\pi^2}{4\pi}\frac{g_s^2}{4\pi}\frac{m_\pi^4}{4m_N^3}\frac{m_N m_\pi}{3\alpha_{00}^+ f_\pi^2}$	$-\frac{g_\pi^2}{4\pi}\frac{g_s^2}{4\pi}\frac{m_\pi^4}{8m_N^3}\left(\frac{1}{3\alpha_{00}^+}\frac{m_N m_\pi}{f_\pi^2}+1\right)$	+0.74

3. NUMERICAL RESULTS

In the present calculations, we use the following parameters: $g_\pi^2/4\pi = 14.4$; another coupling constants from Table III of Ref. [7]; $f_\pi = 93$ MeV; a set of $\{\alpha_{00}^+ = 3.68, g_s = 4.36, m_s = 393 \text{ MeV}\}$ for the $(\pi, 2\pi)$ 3NF [9]; $\Lambda_\pi = 800$ MeV and $\Lambda_\sigma = 1300$ MeV. First, we note that the Argonne V_{18} (AV18) 2NF [10] underbinds the triton (^{3}H) by 0.85 MeV, and the Brazil 2πE (BR_{800}) 3NF [11,12] gives an additional attraction of -1.75 MeV. Thus a repulsive effect is expected to the π-S 3NF to complete the nuclear Hamiltonian.

Calculated values of the ^{3}H energy for the AV18 plus each of the π-S 3NF models are presented in Table 1 as differences from the AV18 calculation. This shows that a π-S 3NF with (positive) V_a-term produces an attractive contribution to the ^{3}H energy, and that with (negative) V_b-term a repulsive contribution, which is consistent with the results given in Ref. [7]. The (π-2π) 3NF consists of a negative V_a-term and a negative V_b-term, and produces a repulsive effect mostly due to the V_a-term.

In order to investigate effects of each term in the π-S 3NF on ND scattering observables, we pick up the following two π-S 3NF models to reproduce the ^{3}H energy together with the AV18 2NF, the BR_{800} 3NF, and a phenomenological spin-orbit type 3NF (SO) [13]:

· The $(\pi\text{-}\sigma)_{Z,PV}$ 3NF as a representative to V_b term;

· The (π-2π) 3NF as a representative to V_a term although it includes a small effect from V_b term. (In this case, we take $\Lambda_\sigma = 800$ MeV.)

The inclusion of the SO 3NF is effective to reproduce the VAPs, but gives only minor effects on the ^{3}H energy and the TAPs at low energies.

Numerical results of Faddeev calculations [14] for the tensor analyzing power $T_{21}(\theta)$ at $E = 3$ MeV and $E = 28$ MeV are presented in Fig. 3, where we plot the experimental data and the results with the 3NFs divided by the AV18 calculations.

For $T_{21}(\theta)$ at 3 MeV, both π-S 3NFs equally tend to cancel the effect due to the 2πE 3NF opposite to the data, but still leave an amount of discrepancy.

At 28 MeV, the 3NFs contribute to $T_{21}(\theta)$ in different ways depending on scattering angles. At scattering angles of 50° to 80°, the calculation with the BR_{800} 3NF and the one with the $\mathrm{BR}_{800} + (\pi, 2\pi)$ 3NFs look consistent with the data. On the other hand, at scattering angles of 90° to 120°, the calculation with the $\mathrm{BR}_{800} + (\pi\text{-}\sigma)_{Z,PV}$ 3NFs as well as the one with only 2NF look consistent with the data.

In Fig. 4 (a), we display results of the transversal $\Delta\sigma_T$ and the longitudinal $\Delta\sigma_L$ asymmetries of the spin dependent total cross sections in $\vec{n} - \vec{d}$ scattering comparing with recent experimental data of $\Delta\sigma_L$ [15]. In Ref. [16], we showed that effects of tensor interactions are prominent in the difference of $\Delta\sigma_T - \Delta\sigma_L$. As expected, differences of tendency in tensor components of the 3NFs are significantly observed in Fig. 4 (b).

4. SUMMARY

We have examined three-nucleon forces arising from the exchange of π and scalar-isoscalar object among three nucleons: π-σ exchange via Z-diagram (V_b-term in Eq. (1)); π-effective 2π exchange (V_a-term, small V_b-term). Both models produce repulsive effects on the ^{3}H energy to compensate strong attraction caused by the 2πE 3NF. Each 3NF affects polarization observables of nucleon-deuteron scattering, $T_{21}(\theta)$ and $\Delta\sigma_T - \Delta\sigma_L$,

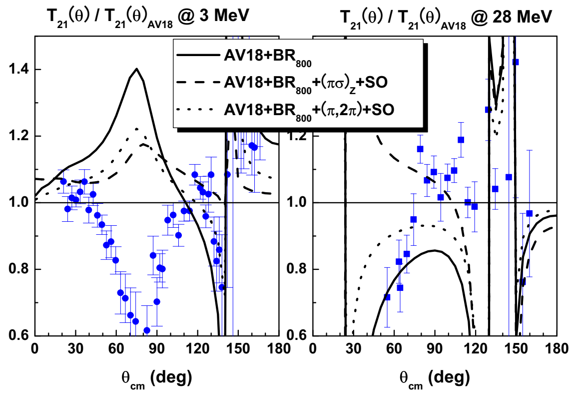

Figure 3. $T_{21}(\theta)$ of pd elastic scattering normalized by the AV18 calculation at $E = 3$ MeV and $E = 28$ MeV. The data are taken from Refs. [1,2] for 3 MeV and from Ref. [3] for 28 MeV.

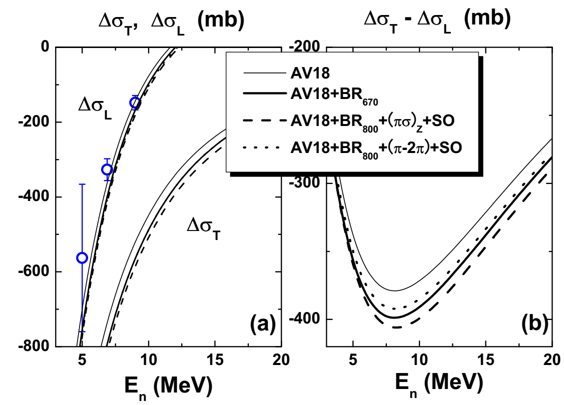

Figure 4. Spin-dependent total cross sections $\Delta\sigma_T$ and $\Delta\sigma_L$ (a), and their difference (b). The data of $\Delta\sigma_L$ are taken from Ref. [15].

in different ways. This shows that further measurements of these observables at some energies provide additional information on three-nucleon forces, which should be included in the nuclear Hamiltonian in addition to the 2πE 3NF.

REFERENCES

1. K. Sagara, *et al.*, Phys. Rev. C **50** (1994) 576.
2. S. Shimizu, *et al.*, Phys. Rev. C **52** (1995) 1193.
3. K. Hatanaka, *et al.*, Nucl. Phys. **A426** (1984) 77.
4. S. Ishikawa, M. Tanifuji, and Y. Iseri, Phys. Rev. C **67** (2003) 061001-R.
5. S. Ishikawa, M. Tanifuji, and Y. Iseri, Proc. of the Seventeenth International IUPAP Conference on Few-Body Problems in Physics. Durham, North Carolina, USA, June 5-10, 2003, edited by W. Glöckle, W. Tornow, (Elsevier, 2004) S61.
6. S. A. Coon, M. T. Peña, and D. O. Riska, Phys. Rev. C **52** (1995) 2925.
7. J. Adam, Jr., M. T. Peña, and A. Stadler, Phys. Rev. C **69** (2004) 034008.
8. C. M. Maekawa and M. R. Robilotta, Phys. Rev. C **57** (1998) 2839.
9. C. M. Maekawa, J. C. Pupin, and M. R. Robilotta, Phys. Rev. C **61** (2000) 064002.
10. R. B. Wiringa, V. G. J. Stoks, and R. Schiavilla, Phys. Rev. C **51** (1995) 38.
11. H. T. Coelho, T. K. Das, and M. R. Robilotta, Phys. Rev. C **28** (1983) 1812.
12. M. R. Robilotta and H. T. Coelho, Nucl. Phys. **A460** (1986) 645.
13. A. Kievsky, Phys. Rev. C **60** (1999) 034001.
14. S. Ishikawa, in preparation.
15. R. D. Foster, *et al.*, Phys. Rev. C **73** (2006) 034002.
16. S. Ishikawa, M. Tanifuji, and Y. Iseri, Phys. Rev. C **64** (2003) 024001.